Gokce Nur Oguz[1]
Department of Mechanical Engineering,
Koç University,
Sarıyer,
Istanbul 34450, Turkey

Senol Piskin[1]
Department of Mechanical Engineering,
Koç University,
Sarıyer,
Istanbul 34450, Turkey

Erhan Ermek
Department of Mechanical Engineering,
Koç University,
Sarıyer,
Istanbul 34450, Turkey

Samir Donmazov
Department of Mechanical Engineering,
Koç University,
Sarıyer,
Istanbul 34450, Turkey

Naz Altekin
Department of Mechanical Engineering,
Koç University,
Sarıyer,
Istanbul 34450, Turkey

Ahmet Arnaz
Department of Cardiovascular Surgery,
Acıbadem Bakırköy Hospital,
Istanbul 34450, Turkey

Kerem Pekkan
Department of Mechanical Engineering,
Koç University,
Rumeli Feneri Campus, Sarıyer,
Istanbul 34450, Turkey
e-mail: kpekkan@ku.edu.tr

Increased Energy Loss Due to Twist and Offset Buckling of the Total Cavopulmonary Connection

The hemodynamic energy loss through the surgically implanted conduits determines the postoperative cardiac output and exercise capacity following the palliative repair of single-ventricle congenital heart defects. In this study, the hemodynamics of severely deformed surgical pathways due to torsional deformation and anastomosis offset are investigated. We designed a mock-up total cavopulmonary connection (TCPC) circuit to replicate the mechanically failed inferior vena cava (IVC) anastomosis morphologies under physiological venous pressure (9, 12, 15 mmHg), in vitro, employing the commonly used conduit materials: Polytetrafluoroethylene (PTFE), Dacron, and porcine pericardium. The sensitivity of hemodynamic performance to torsional deformation for three different twist angles (0 deg, 30 deg, and 60 deg) and three different caval offsets (0 diameter (D), 0.5D, and 1D) are digitized in three dimensions and employed in computational fluid dynamic (CFD) simulations to determine the corresponding hydrodynamic efficiency levels. A total of 81 deformed conduit configurations are analyzed; the pressure drop values increased from 80 to 1070% with respect to the ideal uniform diameter IVC conduit flow. The investigated surgical materials resulted in significant variations in terms of flow separation and energy loss. For example, the porcine pericardium resulted in a pressure drop that was eight times greater than the Dacron conduit. Likewise, PTFE conduit resulted in a pressure drop that was three times greater than the Dacron conduit under the same venous pressure loading. If anastomosis twist and/or caval offset cannot be avoided intraoperatively due to the anatomy of the patient, alternative conduit materials with high structural stiffness and less influence on hemodynamics can be considered.
[DOI: 10.1115/1.4035981]

Keywords: congenital heart disease, Fontan, surgical baffle, arterial buckling, Dacron, PTFE, pericardium blood flow, computational fluid dynamics, hemodynamics, surgical planning, mock-up flow loops

1 Introduction

Congenital heart defects display a large spectrum of severity and impact 8 in 1000 newborns worldwide [1]. Associated surgical repair techniques evolve steadily, which are centered on the palliative total cavopulmonary connection (TCPC), introduced by de Leval et al. [2]. Extracardiac (EC) TCPC is the most common surgical template where the superior vena cava (SVC) is connected to the superior aspect of the right pulmonary artery (RPA) and the inferior vena cava (IVC) is anastomosed to the RPA by using a thin artificial conduit [3]. The typical and most widely used conduit material is polytetrafluoroethylene (PTFE; Gore-Tex, WL Gore & Associates, Newark, NJ). Additional commonly used materials include the porcine pericardium and polyethylene terephthalate (Dacron; DuPont, Wilmington, DE) vascular grafts. Earlier studies have shown that the geometric configuration of TCPC is the main factor in determining the hemodynamic efficiency and the total cardiac output [4–7]. Both in vitro experiments [8–10] and computational fluid dynamics (CFD) studies [11–13] have been conducted previously to investigate the patient-specific flow fields and efficiency in different TCPC surgical templates; however, these studies mostly ignored the mechanical effects of different surgical materials. Using biaxial soft-tissue testing protocols, the mechanical characterization of general surgical materials has been investigated; however, to our knowledge, their effects on the internal flow structures have not been evaluated [14–16].

Due to the growing number of adult patients with "failed" Fontan physiology [17], the hemodynamics of patient-specific conduits of critically ill patients recently gained interest. Particularly, studies focusing pulmonary arteriovenous malformations [18] and the hemodynamics of adult Fontan conversion templates for failed Fontan patients are conducted through computational fluid dynamics [19]. The severely kinked TCPC conduits, associated with patients in critical condition, are not routinely recruited for hemodynamic research studies due to practical or ethical concerns. Nevertheless, in an earlier work we used hypothetical computer-generated configurations to analyze the hemodynamics of TCPC conduit models that were severely compressed and kinked [20]; the results showed that the actual, less-than-optimal TCPC pathways could lead to significant blood flow resistance and thus deserved a systematic analysis. These findings received

[1]G. N. Oguz and S. Piskin contributed equally to this work.

Manuscript received August 1, 2016; final manuscript received January 27, 2017; published online May 3, 2017. Assoc. Editor: Marc Horner.

clinical recognition [21], in spite of the fact that the computer-generated anatomies employed were not realistic and could not provide a conclusive decision. Therefore, the present study is conducted to understand and quantify the effects of realistic but "undesired" Fontan conduit pathways on hemodynamics and energetic performance. In pursuit of this objective, a static mock-up TCPC circuit is designed to replicate and study the mechanically failed IVC morphologies under physiological venous pressures. Commonly used conduit materials are investigated, including the PTFE, Dacron, and porcine pericardium, both computationally (i.e., CFD) and experimentally (i.e., bi-axial testing). The effects of twist angle, caval offset level, and intramural venous pressure on torsional buckling and cardiovascular surgical conduit kink are analyzed in terms of postoperative hemodynamics performance.

The paper is organized as follows: In Sec. 2, static mock-up circuit and three-dimensional (3D) geometry digitization and hemodynamics calculations via CFD are presented. In Sec. 3, the hemodynamic effects of conduit anastomosis configurations on postsurgery performance are determined and compared using the CFD model together with the estimated critical deformation angles of IVC conduits. In Sec. 4, the hemodynamic performance of conduits are compared and analyzed in detail with the limitations of the present study. Finally, suggestions are provided for the specific surgical utility and avenues for possible future studies are presented in Sec. 5.

2 Methodology

2.1 Static Mock-Up Pressure Setup and the 3D Conduit Shapes. Physiological venous pressure levels are applied to the TCPC conduit through a custom mock-up circuit in vitro (Fig. 1). Conduits having 6.5 cm in length and 20 mm in diameter are mounted vertically and positioned as in the actual surgery. The articulated arms of the experimental setup allowed the replication of any intraoperative caval offset and anastomosis twist angles, simultaneously, with an accuracy of ± 1 mm and ± 2.5 deg, respectively.

Caval offset is defined as the distance between the radial centers of SVC and IVC, which is replicated in our mock-up flow loop. Before the Fontan operation, IVC and SVC are approximately aligned for almost all of the patients (except in some cases they will differ especially due to the difference between SVC and IVC diameters). In the experimental setup, the lower articulated arm resembles the IVC inlet and kept fixed at hepatic veins but the upper articulated arm resembles PA anastomosis end and it was free to move "as is" in the surgery. All offsets are replicated according to a hypothetical SVC axis using the upper articulated arm. Likewise, the twist is applied in the desired direction as in Figs. 1 and 2 under the "zero stress state." Offset level and twist angle are used as the main parameters of the geometric configurations in the current study.

Three-dimensional shapes of possible EC TCPC conduit failure modes are replicated under the three intramural pressure levels, 9, 12, and 15 mmHg, covering the healthy (12 mmHg) and progressively failing Fontan disease (9 and 15 mmHg) states. Uncertainty analyses of pressure measurements lead an accuracy of ± 0.1 mmHg. Three caval offset levels of 1 diameter (D), $0.5D$, $0D$, and three relative PA-IVC anastomosis twist angles (0 deg, 30 deg, and 60 deg) are specified, resulting in a total of 81 cases for the three different conduit materials: PTFE, porcine pericardium, and Dacron. The range of twist angles and offset values are decided based on surgeon's experience and cover a broad scope of the possible intraoperative scenarios.

Three-dimensional geometries of all resulting conduit shapes are scanned using an industrial laser scanner (Breuckmann SmartScan R5, Aicon 3D Systems, Braunschweig, Germany) to obtain the deformed surface of the 3D domain for flow simulations under defined static venous pressures.

2.2 Computational Fluid Dynamics Simulations. The 3D geometries of scanned TCPC pathway configurations are reconstructed using GEOMAGIC STUDIO (Raindrop Geomagic Inc., Rock Hill, SC). For brevity, among the 81 deformed configurations, we only present the results of 13 representative kinked conduit geometries in this manuscript (11 PTFE, 1 Dacron, and 1 porcine pericardium). Three of the 13 configurations are specifically identified among 81 states by the pediatric cardiovascular surgeon due to their close resemblance to the conduit geometries that have been observed intraoperatively.

High-quality tetrahedral grids are generated using POINTWISE V16.04 (Pointwise, Inc.) both for an idealized constant diameter

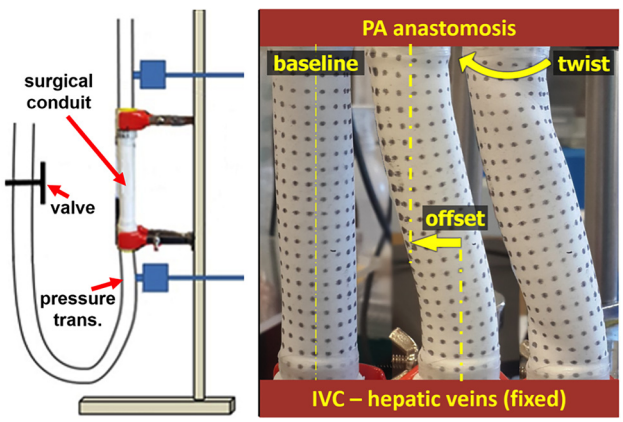

Fig. 1 Schematic static mock-up setup used to acquire three-dimensional nonfunctional conduit shapes (left). The setup is filled with a blood analog fluid. The height of the fluid column is adjusted to apply the required venous pressure level via gravity, and the pressure is measured by taking average of the data from the two pressure transducers. On the right, the PTFE conduit mounted to the setup corresponds to the surface deformations under 9 mmHg pressure. The baseline configuration shown on the left is a straight cylindrical conduit at zero-stress state. The configurations located at the middle and right have caval offset and pulmonary artery anastomosis twist in the specified directions, respectively. The conduit surfaces are marked with a uniform grid to improve three-dimensional laser scanning. IVC: inferior vena cava, PA: pulmonary artery.

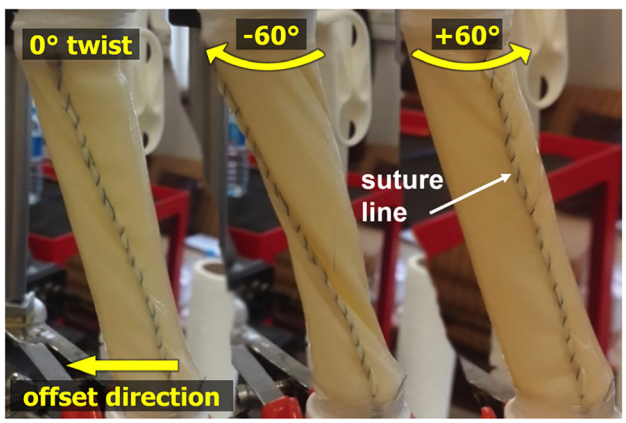

Fig. 2 The deformation of porcine pericardium conduit mounted to the setup with three different configurations under 15 mmHg venous pressure is presented. All three configurations have 1 D caval offset in the direction shown but variable in the anastomosis twist. The left conduit has 0 deg twist angle, middle conduit has 60 deg twist in the clockwise direction, and the right one features 60 deg twist in the counterclockwise direction. Porcine pericardium conduits are produced from a planar tissue segment before the surgery by a pediatric cardiovascular surgeon. Associated "initially straight" suture lines can be identified in all the three plots.

IVC conduit and for reconstructed conduit geometries. The inlet and the outlet of conduits are extended by 5*D* and 10*D*, respectively. For validation simulations, the fully developed flow over ideal constant diameter IVC geometry is employed. Grid dependence test is carried out for three meshes with different element sizes. The computed pressure drop values obtained for those meshes are compared with analytical results calculated using the Hagen–Poiseuille equation; errors are calculated as 2.3%, 0.6%, and 0.3% for 346,233, 568,471, and 1,278,264 elements, respectively. The solver is also validated for correct entrance length prediction. Mesh verification study is also repeated for the most deformed TCPC conduit case by generating different grids (4,576,442, 2,491,254, 1,911,108, 1,233,371, and 762,240 elements). Pressure drops and velocity profiles at these meshes are compared with the finest mesh. Mesh with 1,911,108 elements is chosen as the baseline for all conduit geometries and mesh density is kept constant for all other geometries. For validation, pressure drop of PTFE conduit with 0.5*D* offset, 0 deg twist angle, and under 9 mmHg pressure from our simulation is compared with Fontan conduit pressure drops (IVC section only) from the literature [20] and the results are found to be of the same order.

All simulations are performed by solving 3D steady, laminar, and incompressible Navier–Stokes equations using an open source CFD: SimpleFOAM solver of OpenFOAM.[2] Density and kinematic viscosity of the blood are taken as 1060 kg/m^3 and 3.74×10^{-6} m^2/s, respectively. All simulations converged to a steady-state solution. Residuals are leveled off after 30,000 iterations, but all simulations are run for 50,000 iterations to ensure that convergence is achieved. Pressure and velocity residuals decreased by six orders of magnitude after 50,000 iterations.

To analyze the effect of accordion-like surface of the Dacron conduit on hemodynamics, two additional CFD domains are created with and without surface details having different mesh densities: one without the jagged surface details having 471,259 elements and the other with surface details requiring an extremely fine mesh of 4,576,442 elements. These computations showed no significant difference in pressure drop values and the surface irregularities of the Dacron conduit do not affect the flow field significantly.

Inlet boundary condition for velocity is determined by taking the average of 35 different patient-specific IVC flow Reynolds (Re) numbers, as reported in literature, which resulted in 557 ± 258 [22–25]. Parabolic velocity inlet (maximum velocity of 0.19 m/s) and constant outlet pressure boundary conditions are specified. The hydrodynamic pressure drop between the inlet and outlet of the conduit is calculated and compared for all selected geometries to represent hydrodynamic energy loss. All of the pressure drop values reported in Sec. 3 are relative to the idealized straight constant diameter IVC conduit (with a length of 6.5 cm and a diameter of 20 mm) pressure drop. The baseline Re number employed in this manuscript results in a pressure drop of 1.96 Pa under Poiseuille flow condition for the same conduit length. The differences in computed pressure drop values are calculated using Eq. (1), which read as

$$\%\ \text{Pressure Drop Difference} = \frac{(\Delta P - \Delta P_{\text{Poiseuille}})}{\Delta P_{\text{Poiseuille}}} \times 100 \quad (1)$$

Integrated control volume energy balance equation is used to compute power losses ($\dot{E}_{\text{loss}}$) across the conduit

$$\dot{E}_{\text{loss}} = \sum_{\text{Inlets}} P_i \cdot Q_i - \sum_{\text{Outlets}} P_i \cdot Q_i \quad (2)$$

where P_i and Q_i are total pressures and volumetric flow rate, respectively. For a single inlet and single outlet conduit, the flow rate is constant and thus the pressure drop and energy loss are related linearly.

[2]www.openfoam.org

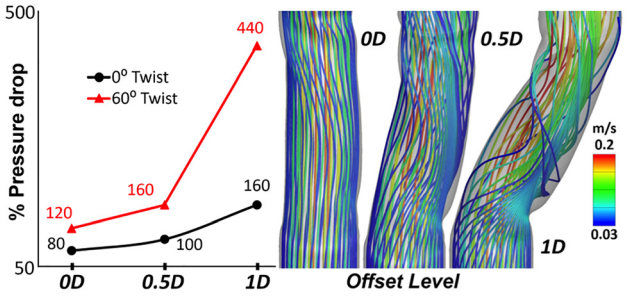

Fig. 3 For three caval offset levels, the differences in computed pressure drop values are presented under 15 mmHg intramural venous pressure (left plot). In these experiments, PTFE conduits with 0 deg and 60 deg twist angles are used. Reported percent differences are calculated relative to the straight ideal conduit at the same flow conditions, which results in a pressure drop of 1.96 Pa under Poiseuille flow condition for the same conduit length. Corresponding IVC flow streamlines are presented on the right, shaded with the local velocity magnitude. These CFD simulations correspond to PTFE under 60 deg twist angle, 15 mmHg venous pressure at 0*D*, 0.5*D*, and 1*D* offset levels displayed from left to right.

3 Results

3.1 Caval Offset Level. In this section, the results presented are those that correspond to the highest intramural venous pressure of 15 mmHg and PA anastomosis twist angles of 0 deg and 60 deg (Fig. 3). For offset level parameter analysis, other twist and venous pressure values provided similar trends and are not included here for the sake of brevity.

A finite caval offset generates a characteristic surface deformation pattern on the initially perfectly circular smooth conduit. These deformed surface patterns resemble a kinked vascular geometry in the direction of the offset and result in local flow area reduction. Corresponding changes in surface shapes, flow streamlines, and pressure drop changes for different offset levels and two different twist angles are illustrated in Fig. 3. All configurations resulted in significantly higher energy losses compared to the ideal uniform diameter conduit due to surface irregularities. Among these three cases, the 0.5*D* offset configuration is identified as a realistic conduit shape by practicing pediatric cardiovascular surgeons due to its close resemblance to intraoperatively observed shapes. For twist angle of 60 deg, the pressure drop difference for 0.5*D* offset resulted 1.3 times more than 0*D* offset case while the case with 1*D* resulted 3.6 times more than the 0*D* offset pressure drop, demonstrating a nonlinear behavior. The pressure differences for twist angle of 0 deg are not dramatic but follow a similar path to that of 60 deg twist angle. As the offset level increases, the laminar flow starts to become disturbed and evolves into a rotating flow due to the curvature of the conduit surface. Initial vortex formation is visible, especially at buckled regions of the 1*D* offset configuration.

3.2 PA-IVC Anastomosis Twist Angle. Similarly, the effect of twist at the PA anastomosis site is studied for three torsional angles, corresponding to 0 deg, 30 deg, and 60 deg for PTFE conduit at constant 0*D* offset and 12 mmHg intramural pressure level (Fig. 4). Among these three cases, the 30 deg and 60 deg twist angle configurations are identified as realistic conduit shapes by practicing pediatric cardiovascular surgeons due to their close resemblance to intraoperatively observed geometries. All configurations resulted in higher energy losses, up to 110% compared to the ideal uniform diameter conduit, demonstrating the significance of deformation caused by twist. A consistently linear relationship between the pressure drop values and twist angle level is observed. Thus, if needed, the pressure drop differences for higher twist angle levels can be extrapolated from these data. Alterations

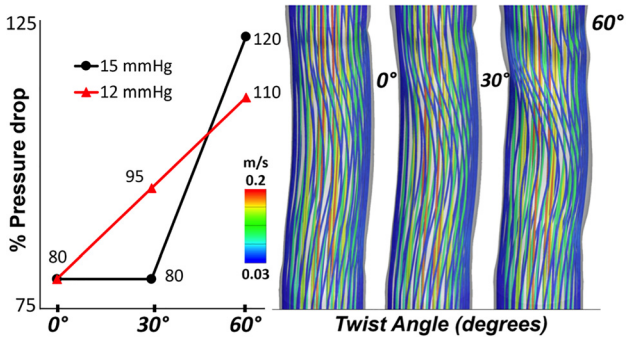

Fig. 4 For the three PA-IVC anastomosis twist angle levels, the differences in computed pressure drop values are presented corresponding to the PTFE under 0*D* offset configuration subjected to 12 mmHg and 15 mmHg venous pressure (left plot). Reported values are in percentage and are relative to the straight conduit at the same flow conditions, which results in a pressure drop of 1.96 Pa under Poiseuille flow condition for the same conduit length. Corresponding IVC flow streamlines are presented on the right, shaded with the local velocity magnitude. These CFD simulations correspond to PTFE under 0*D* offset, 12 mmHg venous pressure with 0 deg, 30 deg, and 60 deg twist angle displayed from left to right.

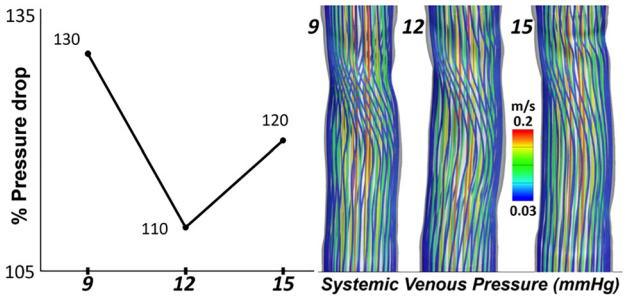

Fig. 5 For the three internal venous pressure levels, the differences in computed pressure drop values are presented corresponding to the PTFE under 0*D* offset, 60 deg twist angle configuration (left plot). Reported values are in percentage and are relative to the straight conduit at the same flow conditions, which results in a pressure drop of 1.96 Pa under Poiseuille flow condition for the same conduit length. Corresponding IVC flow streamlines are presented on the right, shaded with the local velocity magnitude. These CFD simulations correspond to PTFE under 0*D* offset, 60 deg twist angle with 9, 12, and 15 mmHg systemic venous pressure displayed from left to right.

in the twist angle resulted in a moderate effect on pressure drop; a 60 deg twist angle increases the pressure drop 1.35-fold compared to a 0 deg twist angle. Twisting the anastomosis region deforms the conduit and the flow starts to rotate at the opposite direction of the twist upon entering the PA. Similar to the offset level, increasing the twisting angle increases the buckling (i.e., deformation) and thus the vorticity in of the flow, which would contribute to power loss. To compare different venous pressure effects, 15 mmHg results are also presented in Fig. 4. Although the pressure drop difference tends to increase by twist angle, the 30 deg does not cause any significant change with respect to 0 deg. This could be due to the resistance of the conduit under high venous pressure levels.

In vitro experiments showed that relative directions of twist and offset are critical for the resulting conduit surface irregularities. This is illustrated clearly in Fig. 2 for the porcine pericardium conduit. If the offset and twist are applied in the same direction, the severity of buckling increases, while if the offset and twist are in reverse directions, this reduces the severity of the buckling and causes a relatively larger pathway cross-sectional area and smooth surface form. This effect is relatively less common for the PTFE and Dacron conduits due to their higher elastic modulus. Porcine pericardium shows less resistance to offset and twist, especially around the suture line, while Dacron and PTFE have uniform cylindrical structure; this may be an additional reason for the observed differences in their behavior with respect to twist/offset direction.

3.3 Systemic Venous Pressure. We hypothesized that increasing intramural venous pressures would increase the inner vessel diameter and smoothen the surface irregularities caused by twist and offset, consequently reducing pressure drop levels. In order to analyze the effect of venous pressure on conduit buckling, three different pressure loads (9 mmHg, 12 mmHg, and 15 mmHg) at 30 deg PA twist angle and 0*D* offset are specified for the PTFE conduit (Fig. 5). For these pressure loads, only a 20% change in the pressure drop levels are observed, possibly due to the nonlinearity of the material response.

From 9 mmHg to 12 mmHg, due to the increased systemic venous pressure level, the severity of the conduit buckling decreased and the pressure drop reduced by around 20%. This is an expected result since the higher pressure would enlarge the cross-sectional area and thus prevent the closing of the conduit. However, due to the complexity of the deformed conduit, changing systemic venous pressure from 12 mmHg to 15 mmHg increased the throat diameter beyond the nominal diameter, which further resulted in flow separation (as can be seen in aneurysms) and caused an increase in the pressure drop. A detailed examination of the conduit throughout the axial direction showed that a local abrupt decrease in cross-sectional area caused by buckled geometry and high pressure resulted in higher-pressure drop values between 12 mmHg and 15 mmHg. Buckling causes arbitrary deformation (i.e., nonlinear), and the cross-sectional area fluctuates along the centerline. Pressure change does not have a substantial effect on the vortex formation, although vorticity decreases slightly as the pressure increases from 9 mmHg to 15 mmHg, as can be observed in Fig. 5. The flow circulation presented in the figures is initiated due to a 60 deg twist angle.

The minimum anastomosis angle that results in a visually identifiable conduit deformation is defined as the "critical deformation angle." This angle is determined from mock-up experiments through visual observations and is found to be different for PTFE, Dacron, and porcine pericardium. A linear relation between

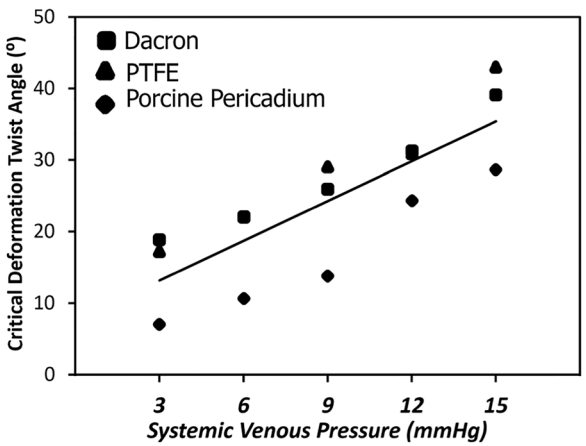

Fig. 6 Critical deformation angle with respect to the increase in systemic venous pressure is presented for the three different conduit materials with 0*D* offset: Dacron, PTFE, and porcine pericardium. Critical deformation angle is defined as the first visually detectable surface wrinkling (as the anastomosis twist is increased slowly) from our mock-up setup.

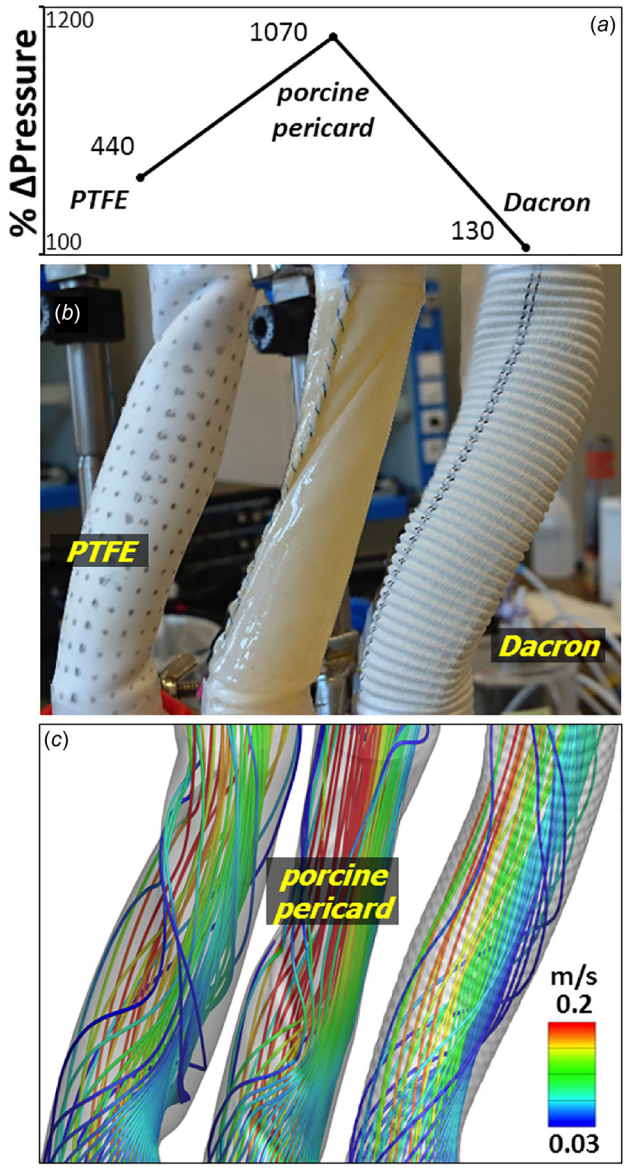

Fig. 7 For the three conduit materials studied, the differences in computed pressure drops are presented corresponding to the 1*D* offset and 60 deg twist angle configuration subjected to 15 mmHg venous pressure (*a*). Reported values are in percentage and are relative to the straight conduit at the same flow conditions, which results in a pressure drop of 1.96 Pa under Poiseuille flow condition for the same conduit length. Snapshots of the PTFE, porcine pericardium, and Dacron conduits obtained from the mock-up setup are displayed corresponding to the 1*D* offset, 60 deg twist angle configuration subjected to 15 mmHg venous pressure from left to right (*b*). Corresponding three-dimensional conduit flow pathways are shaded with the local velocity magnitude in m/s for PTFE, pericardium, and Dacron (from left to right) under 1*D* offset, 60 deg twist angle and 15 mmHg venous pressure condition (*c*). The surface irregularities of the Dacron conduit that are resolved by the CFD model are also visible in (*c*). ΔPressure refers to the percent pressure drop difference.

internal pressure and critical deformation angle is observed and obtained by least square fitting for all three materials (Fig. 6). It can also be interpreted from the relationship that as the internal pressure increases, it gets harder to deform the conduit.

3.4 Conduit Material. The effects of different conduit materials on flow characteristics are also analyzed. The tests at 15 mmHg venous pressure and 60 deg PA twist angle with 1*D* offset are performed for three conduit materials: PTFE, Dacron, and porcine pericardium (Fig. 7). Material change resulted in up to a tenfold difference in pressure drop and an associated substantial difference in surface deformation, as shown in Fig. 7. The pressure drop values for PTFE are almost three times greater than for the Dacron conduit, while porcine pericardium values are eight times greater than the Dacron conduit.

To elucidate these differences, the gross mechanical properties of these three materials should be taken into consideration. Poisson's ratio for PTFE, porcine pericardium, and Dacron porcine is 0.31, 0.42, and 0.39, respectively, and Young's modulus is 1.807, 1.050, and 2.601, respectively [26]. Porcine pericardium has the lowest stiffness, which resulted in excessive deformation on conduit surface and a decrease in cross-sectional area. When offset and twist are applied to the conduit, deformations increased, particularly around the stitch area. Furthermore, in the pericardium model, flow gained momentum in the radial direction due to narrowing, and recirculation zones are augmented, which correlates with the highest observed pressure drop. For the PTFE material, surface deformation is initiated proximal to the conduit's anastomosis locations, which is different than the Dacron and porcine pericardium grafts. While all materials are compressible with a Poisson's ratio lower than 0.42, PTFE is significantly more compressible, with a Poisson's ratio of 0.31. Finally, Dacron was found to be the stiffest material among the three conduit samples and did not show significant visible surface buckling in vitro due to its accordion-like folding structure. Thus, the Dacron conduit has the lowest centerline velocity and lowest pressure drop among the three conduit materials considered.

4 Discussion

Buckling in arteries and veins as the upshot of vascular instability plays a substantial role in the formation of several cardiovascular pathologies [27]. In the current study, an in vitro analysis of surgical configurations with the potential for buckling has been conducted for the first time in literature, to our knowledge. Even though the patient-specific geometries of the failed Fontan configurations have not been studied in the previous literature extensively, our study's initial results show that the buckling and kinking modes could be major contributors to the excessive energy loss levels.

An important factor causing energy loss is the local flow separation observed in severely deformed conduits. Although straight conduits feature uniform flow streamlines, the formation of local vortices and disturbed flow structures are observed for both the offset and twisted conduits. Severely twisted conduit walls also have the potential to direct and generate the helical flow. In general, increasing the twist and offset levels resulted in greater pressure drops and flow separation throughout the conduit. An outlier is observed between the 0.5*D* and 1*D* offset configurations, as displayed in Fig. 3; a 1*D* caval offset level resulted in a pressure drop up to three times greater than the no offset case. Due to the nonlinear relation between offset level and pressure drop, higher offset levels produced ambiguous but high pressure drops (results not included for brevity). Vortex formation is observed at the buckled regions of the conduit as the offset level increases.

Relative anastomosis twist and caval offset are the main parameters that affect the level of conduit deformation and tortuosity. Considering all of the 81 in vitro IVC conduit shapes acquired from our mock-up circuit, calculated pressure drop differences range from 80% to 1070% higher than the straight conduit. These 81 cases not only include a number of highly deformed cases, but also include the realistic cases identified by pediatric cardiovascular surgeons. These realistic cases lead to moderate pressure difference values, ranging from 110% to 160%. It should be noted that the intraoperative conduit configurations studied in this manuscript correspond to the early postoperative stage and may change during the long-term postoperative period.

The contribution of the IVC section to the total TCPC hydrodynamic energy budget is significant; the IVC section contributes around 20% to the total flow energy loss in a functional TCPC pathway [3,4,9,24,25,28,29]. However, IVC flow can further increase up to five times under exercise conditions [30], particularly for leg exercise, as this primarily increases the IVC flow. It is also expected that IVC energy loss would be higher in an actual patient-specific TCPC geometry [4,9], although energy losses at the downstream PAs could also increase such that the relative contribution of the IVC conduit may not necessarily increase for some patients. These estimates are conservative, as they are based on a constant vessel diameter Poiseuille flow assumption, whereas TCPC junction features complex flow structures; IVC flow will interact with the downstream PA circulation through a highly nonlinear physics, which would likely to lead higher energy losses at the IVC.

For the first time in literature, we show that caval offset can indeed cause significant surface deformation that leads to substantially lower hemodynamic performance. Although increasing the twist angle also increased pressure drop levels and vorticity, it is concluded that the effect of twisting is not as important as offsetting on hemodynamics. There is at most a 1.35-fold increase in pressure drop between 0 deg and 60 deg twist angle, while there is a 3.6-fold increase in pressure drop between 0*D* and 1*D* offset level. Furthermore, the initial vortex formation is visible during twisting to 60 deg, but there is only a slight change between 30 and 60 deg compared to the offset effect.

Although there is no direct analytical relation binding the internal pressure to the critical deformation angle, our results suggest that increasing blood pressure results in an additional positive moment, which, in turn, linearly increases the critical deformation angle and reduces buckled regions on the surface. The additional positive moment is probably produced due to unsymmetrical material surface and likely increases the material's resistivity to the twist. As the internal venous pressure increases, surgeons would have a higher range of twist angles at which they could safely anastomose the conduit without any deformation. Since in theory buckling instability starts without any visible surface deformation, we have also defined a visual critical deformation angle parameter in our study. This angle corresponds to the first "visible" initiation of surface deformation. Even though the critical deformation angle is a subjective parameter, it will still be useful intraoperatively establishing the relation between our quantitative pressure drop measurements.

Although the increased venous pressure enlarges the conduit diameter and smoothens buckling irregularities, which leads to reduced hydrodynamic energy loss at the IVC section, high pulmonary vascular resistance (PVR) is absolutely not desired due to its detrimental effects for the single-ventricle physiology. High PVR results in venous remodeling and would lead to multi-organ failure. As such, among the materials studied, the Dacron conduit was found to be the most structurally stable design for both twist and offset due to the higher bending stiffness of its jagged cross section, as compared to PTFE and porcine pericardium conduits. Since the Dacron conduit did not show any narrowing due to buckling, the Dacron conduit experiences the least pressure drop during blood flow among the three materials considered. PTFE conduit has a pressure drop up to three times greater than the Dacron conduit. Porcine pericardium conduit has the worst pressure drop performance, with an eightfold increase compared to the Dacron conduit; this is due to porcine pericardium's highly deformable surface and narrowed cross section. Dacron offers a partial solution to conduit deformation in terms of lower energy loss but additional criteria should be taken into consideration. For example, the jagged surface of the Dacron graft may promote thrombosis formation especially during the early postoperative period, compared to the smooth PTFE. Material designs like Dacron are the first step toward improved conduit rigidity but there may be advanced material configurations, having smooth inner surfaces that can still resist buckling, through controlled directional microstructure [31–33]. Likewise, the stiffness of the material is critical, since the materials with higher stiffness resulted in lower pressure drop values. However, less stiff materials will have similar properties with the native vessel resulting smoother stress transitions. The mechanical response of the conduit material is substantial for energy loss and should be considered during the presurgery planning phase.

There are a number of limitations to the present work. While we utilized flexible end points and holders as much as possible in our mock-up circuit, the actual suture lines at the PA anastomosis region are probably more flexible and could thus generate a wider variety of shapes than the circular shape imposed due to our experimental setup. In addition, for an actual TCPC pathway, common atrium and external ventricle surfaces provide additional structural stability and compression effects, which are not replicated in the mock-up circuit. However, based on our clinical experience, this factor would play a secondary role and our results still illustrate the significance of Fontan pathways. In addition, materials are assumed to be homogeneous, isotropic, and linear elastic; however, employing orthotropic hyperplastic models would give more precise information about the materials' responses. The assumption of planar cross-sectional area might also be a weak claim since it may not represent the real patient-specific conduit irregularities.

The lowest pressure drop difference calculated among 81 configurations is 75% for the case with no twist and offset under 9 mmHg pressure load. Pressure drop increase is associated with multiple sources. The ideal geometry used for the pressure-drop comparison has a constant inner diameter, perfectly smooth surface obtained from the CAD software. In contrast, the in vitro measured conduit surfaces are not perfectly smooth through the conduit length. These small irregularities may also be exacerbated due to slight gravitational effects caused by the test setup and influence the ideal pressure drop values. Another increase in pressure drop could be due to the connectors located at the inlet and outlet of the conduit. Although these connections have exactly the same diameter with the medical conduit, a slight disturbance at the transition region between the conduit and the connectors is unavoidable. Still, we believe that the latter effect is minor due to the relatively smooth transition at the vicinity of the connectors ensured during experiments. The thickness of grafts varies between 0.4 and 0.9 mm for different conduit materials. We take the outer diameter of the grafts as nominal value and adjust the diameter of the holder arm by taking into consideration the thickness of the materials.

According to our observations from the mock-up circuit, porcine pericardium and Dacron conduits resulted in surface leakage at a rate of 3 and 12.5 ml/min, respectively, due to their porous and textile structure. For the Dacron conduit, we eliminated surface leakage by introducing a thin layer of water resistant polymer film. Pericardium leakage is concentrated on the suture line, while the PTFE conduit did not show any leakage. Leakage pores may be significant during early post-op if negative intramural pressure occurs (ex: heart-lung machine), as they have the potential to introduce microbubbles into the venous system.

In this study, CFD simulations were realized for rigid wall and steady state flow conditions; however, the geometries were reconstructed from scanned data in a pressurized state under average IVC flow conditions. Rigid wall assumptions are appropriate for this study since, particularly for the IVC section, wall motion should be less significant for the realistic in vivo venous flow conditions. Since blood flow velocity is relatively low, non-Newtonian effects are important in terms of velocity profile. We simulated all cases under Newtonian viscosity assumption and compared pressure drops between these models. The comparison is thus still meaningful, even though we did not use a non-Newtonian model.

The full TCPC geometry together with a rapid-prototype single-ventricle should be considered in the future experiments. In this study, we focused only on the IVC section, as otherwise the

full model would excessively complicate both the experimental and the computational model. One main reason for this approach is the need to employ native PA vessels in the experimental setup, which was almost impossible. Furthermore, we intended to isolate and study the influence of surface deformations only at the IVC section; we thought that the deformations of the full model will be very complex and would not help us much to identify and illustrate the physical response clearly. The kink or twist degree of the conduits can also be identified via standard cardiac imaging post-operatively and their severity can be assessed. From the image data, the pressure drop in the conduit can be estimated, which may be important for the re-operation decisions of severely deformed conduits.

5 Conclusions

The major mode of flow restriction in compressed and kinked TCPC conduits is associated with conduit buckling, which can occur due to its geometric configuration and abnormal blood flow inside the conduit. The relative PA anastomosis twist angle and caval offset levels are the essential geometric factors that affect the severity of conduit buckling. Systemic venous pressure also alters the conduit geometry and thus the buckling severity. Apparently, the primary factor that contributes to the pressure drop is the narrowing of the vessel due to buckling or offset kink at several regions of the conduit. Another factor causing the pressure drop is disturbance of the blood flow due to nonsmooth pathway as well as converging—diverging wall contours. This imbalance in wall contours lead to local flow separation and sharp velocity/pressure changes, as in arterial stenosis contributing to the total hydrodynamic energy budget. It is very important to keep the offset level and torsion of the conduit as low as possible and to hold the conduit as straight as possible during surgery; otherwise, the conduit could cause up to a tenfold energy loss compared to an idealized circular pipe conduit. On the other hand, the value of caval offset in reducing the energy loss is still important. The present study indicated a precaution for the utilization of excessive caval offset, which would reduce performance especially if the twist and offset exist together, in a directionally dependent way. Furthermore, the material properties of the conduit substantially change the buckling level and shape under the same twist, offset and pressure. Thus, if the surgical practice cannot prevent slight twist and/or offset due to the anatomy of the patient, altering the surgical conduit material can lead to lower pressure drop levels in the pathway. Dacron conduit was found to be the best material in terms of energy loss among the three conduits investigated and could be chosen in these terms but other factors such as high thrombosis formation risk should be taken into consideration. For future work, novel conduit structures that are not prone to severe buckling could be proposed based on the material properties and critical buckling angles presented in the current study.

Acknowledgment

Funding was provided by grants from the European Research Council (ERC) Proof of Concept Grant *KidsSurgicalPlan*, ERC Starting Grant 307460 and TUBITAK 1003 priority-research program.

References

[1] Boneva, R. S., Botto, L. D., Moore, C. A., Yang, Q., Correa, A., and Erickson, J. D., 2001, "Mortality Associated With Congenital Heart Defects in the United States: Trends and Racial Disparities, 1979–1997," Circulation, **103**(19), pp. 2376–2381.

[2] de Leval, M. R., Kilner, P., Gewillig, M., and Bull, C., 1998, "Total Cavopulmonary Connection: A Logical Alternative to Atriopulmonary Connection for Complex Fontan Operations. Experimental Studies and Early Clinical Experience," J. Thorac. Cardiovasc. Surg., **96**(5), pp. 682–695.

[3] Liu, Y., Pekkan, K., Jones, S. C., and Yoganathan, A. P., 2004, "The Effects of Different Mesh Generation Methods on Computational Fluid Dynamic Analysis and Power Loss Assessment in Total Cavopulmonary Connection," ASME J. Biomech. Eng., **126**(5), pp. 594–603.

[4] Ryu, K., Healy, T. M., Ensley, A. E., Sharma, S., Lucas, C., and Yoganathan, A. P., 2001, "Importance of Accurate Geometry in the Study of the Total Cavopulmonary Connection: Computational Simulations and In Vitro Experiments," Ann. Biomed. Eng., **29**(10), pp. 844–853.

[5] Hosein, R. B., Clarke, A. J., McGuirk, S. P., Griselli, M., Stumper, O., De Giovanni, J. V., Barron, D. J., and Brawn, W. J., 2007, "Factors Influencing Early and Late Outcome Following the Fontan Procedure in the Current Era. The 'Two Commandments'?," Eur. J. Cardiothorac. Surg., **31**(3), pp. 344–352.

[6] Pekkan, K., Kitajima, H. D., de Zelicourt, D., Forbess, J. M., Parks, W. J., Fogel, M. A., Sharma, S., Kanter, K. R., Frakes, D., and Yoganathan, A. P., 2005, "Total Cavopulmonary Connection Flow With Functional Left Pulmonary Artery Stenosis: Angioplasty and Fenestration In Vitro," Circulation, **112**(21), pp. 3264–3271.

[7] Walker, P. G., Howe, T. T., Davies, R. L., Fisher, J., and Watterson, K. G., 2000, "Distribution of Hepatic Venous Blood in the Total Cavo-Pulmonary Connection: An In Vitro Study," Eur. J. Cardiothorac. Surg., **17**(6), pp. 658–665.

[8] Gerdes, A., Kunze, J., Pfister, G., and Sievers, H. H., 1999, "Addition of a Small Curvature Reduces Power Losses Across Total Cavopulmonary Connections," Ann. Thorac. Surg., **67**(6), pp. 1760–1764.

[9] Ensley, A. E., Lynch, P., Chatzimavroudis, G. P., Lucas, C., Sharma, S., and Yoganathan, A. P., 1999, "Toward Designing the Optimal Total Cavopulmonary Connection: An In Vitro Study," Ann. Thorac. Surg., **68**(4), pp. 1384–1390.

[10] Sharma, S., Goudy, S., Walker, P., Panchal, S., Ensley, A., Kanter, K., Tam, V., Fyfe, D., and Yoganathan, A., 1996, "In Vitro Flow Experiments for Determination of Optimal Geometry of Total Cavopulmonary Connection for Surgical Repair of Children With Functional Single Ventricle," J. Am. Coll. Cardiol., **27**(5), pp. 1264–1269.

[11] de Leval, M. R., Dubini, G., Migliavacca, F., Jalali, H., Camporini, G., Redington, A., and Pietrabissa, R., 1996, "Use of Computational Fluid Dynamics in the Design of Surgical Procedures: Application to the Study of Competitive Flows in Cavo-Pulmonary Connections," J. Thorac. Cardiovasc. Surg., **111**(3), pp. 502–513.

[12] Dubini, G., de Leval, M. R., Pietrabissa, R., Montevecchi, F. M., and Fumero, R., 1996, "A Numerical Fluid Mechanical Study of Repaired Congenital Heart Defects. Application to the Total Cavopulmonary Connection," J. Biomech., **29**(1), pp. 111–121.

[13] Migliavacca, F., de Leval, M. R., Dubini, G., Pietrabissa, R., and Fumero, R., 1999, "Computational Fluid Dynamic Simulations of Cavopulmonary Connections With an Extracardiac Lateral Conduit," Med. Eng. Phys., **21**(3), pp. 187–193.

[14] Bustos, C. A., García-Herrera, C. M., and Celentano, D. J., 2016, "Mechanical Characterisation of Dacron Graft: Experiments and Numerical Simulation," J. Biomech., **49**(1), pp. 13–18.

[15] Tremblay, D., Zigras, T., Cartier, R., Leduc, L., Butany, J., Mongrain, R., and Leask, R. L., 2009, "A Comparison of Mechanical Properties of Materials Used in Aortic Arch Reconstruction," Ann. Thorac. Surg., **88**(5), pp. 1484–1491.

[16] Lee, M. C., Fung, Y. C., Shabetai, R., and LeWinter, M. M., 1987, "Biaxial Mechanical Properties of Human Pericardium and Canine Comparisons," Am. J. Physiol., **253**(1), pp. H75–H82.

[17] Ohuchi, H., 2016, "Adult Patients With Fontan Circulation: What We Know and How to Manage Adults With Fontan Circulation?," J. Cardiol., **68**(3), pp. 181–189.

[18] Sundareswaran, K. S., de Zelicourt, D., Sharma, S., Kanter, K. R., Spray, T. L., Rossignac, J., Sotiropoulos, F., Fogel, M. A., and Yoganathan, A. P., 2009, "Correction of Pulmonary Arteriovenous Malformation Using Image-Based Surgical Planning," JACC Cardiovasc. Imaging, **2**(8), pp. 1024–1030.

[19] Hong, H., Dur, O., Zhang, H., Zhu, Z., Pekkan, K., and Liu, J., 2013, "Fontan Conversion Templates: Patient-Specific Hemodynamic Performance of the Lateral Tunnel Versus the Intraatrial Conduit With Fenestration," Pediatr. Cardiol., **34**(6), pp. 1447–1454.

[20] Yoshida, M., Menon, P. G., Chrysostomou, C., Pekkan, K., Wearden, P. D., Oshima, Y., Okita, Y., and Morell, V. O., 2013, "Total Cavopulmonary Connection in Patients With Apicocaval Juxtaposition: Optimal Conduit Route Using Preoperative Angiogram and Flow Simulation," Eur. J. Cardiothorac. Surg., **44**(1), pp. e46–e52.

[21] de Leval, M. R., 2013, "Re: Total Cavopulmonary Connection in Patients With Apicocaval Juxtaposition: Optimal Conduit Route Using Preoperative Angiogram and Flow Simulation," Eur. J. Cardiothorac. Surg., **44**(1), p. e52.

[22] Dasi, L. P., Krishnankuttyrema, R., Kitajima, H. D., Pekkan, K., Sundareswaran, K. S., Fogel, M., Sharma, S., Whitehead, K., Kanter, K., and Yoganathan, A. P., 2009, "Fontan Hemodynamics: Importance of Pulmonary Artery Diameter," J. Thorac. Cardiovasc. Surg., **137**(3), pp. 560–564.

[23] Haggerty, C. M., de Zelicourt, D. A., Restrepo, M., Rossignac, J., Spray, T. L., Kanter, K. R., Fogel, M. A., and Yoganathan, A. P., 2012, "Comparing Pre- and Post-Operative Fontan Hemodynamic Simulations: Implications for the Reliability of Surgical Planning," Ann. Biomed. Eng., **40**(12), pp. 2639–2651.

[24] Khiabani, R. H., Restrepo, M., Tang, E., De Zélicourt, D., Sotiropoulos, F., Fogel, M., and Yoganathan, A. P., 2012, "Effect of Flow Pulsatility on Modeling the Hemodynamics in the Total Cavopulmonary Connection," J. Biomech., **45**(14), pp. 2376–2381.

[25] Tang, E., Haggerty, C. M., Khiabani, R. H., de Zelicourt, D., Kanter, J., Sotiropoulos, F., Fogel, M. A., and Yoganathan, A. P., 2013, "Numerical and Experimental Investigation of Pulsatile Hemodynamics in the Total Cavopulmonary Connection," J. Biomech., **46**(2), pp. 373–382.

[26] Donmazov, S., Piskin, S., Ermek, E., and Pekkan, K., 2016, "Mechanical Characterization and Torsional Buckling Effects of Vascular Conduits," J. Mech. Behav. Biomed. Mater. (to be submitted).
[27] Garcia, J. R., Lamm, S. D., and Han, H. C., 2013, "Twist Buckling Behavior of Arteries," Biomech. Model. Mechanobiol., **12**(5), pp. 915–927.
[28] Desai, K., Haggerty, C. M., Kanter, K. R., Rossignac, J., Spray, T. L., Fogel, M. A., and Yoganathan, A. P., 2013, "Haemodynamic Comparison of a Novel Flow-Divider Optiflo Geometry and a Traditional Total Cavopulmonary Connection," Interact. Cardiovasc. Thorac. Surg., **17**(1), pp. 1–7.
[29] Healy, T. M., Lucas, C., and Yoganathan, A. P., 2001, "Noninvasive Fluid Dynamic Power Loss Assessments for Total Cavopulmonary Connections Using the Viscous Dissipation Function: A Feasibility Study," ASME J. Biomech. Eng., **123**(4), pp. 317–324.
[30] Whitehead, K. K., Pekkan, K., Kitajima, H. D., Paridon, S. M., Yoganathan, A. P., and Fogel, M. A., 2007, "Nonlinear Power Loss During Exercise in Single-Ventricle Patients After the Fontan: Insights From Computational Fluid Dynamics," Circulation, **116**(11), pp. I165–I171.
[31] Montini-Ballarin, F., Calvo, D., Caracciolo, P. C., Rojo, F., Frontini, P. M., Abraham, G. A., and Guinea, G. V., 2016, "Mechanical Behavior of Bilayered Small-Diameter Nanofibrous Structures as Biomimetic Vascular Grafts," J. Mech. Behav. Biomed. Mater., **60**, pp. 220–233.
[32] Pashneh-Tala, S., MacNeil, S., and Claeyssens, F., 2015, "The Tissue-Engineered Vascular Graft-Past, Present, and Future," Tissue Eng., Part B, **22**(1), pp. 68–100.
[33] Tan, Z., Wang, H., Gao, X., Liu, T., and Tan, Y., 2016, "Composite Vascular Grafts With High Cell Infiltration by Co-Electrospinning," Mater. Sci. Eng., C, **67**, pp. 369–377.